

## Accepted Manuscript

Synthesis, biological evaluation and molecular docking study of 1,2,3-*H*-triazoles having 4*H*-pyrano[2,3-*d*]pyrimidine as potential *Mycobacterium tuberculosis* protein tyrosine phosphatase B inhibitors

Nguyen Dinh Thanh, Do Son Hai, Nguyen Thi Thu Ha, Do Tien Tung, Cao Thi Le, Hoang Thi Kim Van, Vu Ngoc Toan, Duong Ngoc Toan, Le Hai Dang

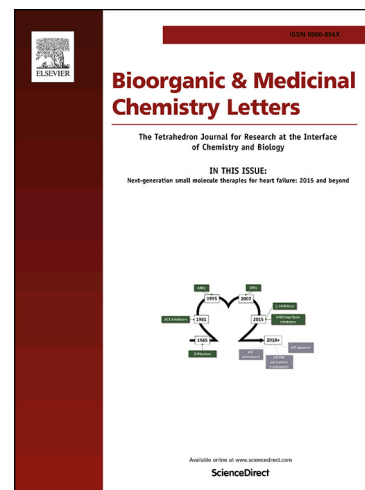
PII: S0960-894X(18)30945-4  
DOI: <https://doi.org/10.1016/j.bmcl.2018.12.009>  
Reference: BMCL 26178

To appear in: *Bioorganic & Medicinal Chemistry Letters*

Received Date: 23 October 2018  
Revised Date: 26 November 2018  
Accepted Date: 4 December 2018

Please cite this article as: Thanh, N.D., Hai, D.S., Ha, N.T.T., Tung, D.T., Le, C.T., Van, H.T.K., Toan, V.N., Toan, D.N., Dang, L.H., Synthesis, biological evaluation and molecular docking study of 1,2,3-*H*-triazoles having 4*H*-pyrano[2,3-*d*]pyrimidine as potential *Mycobacterium tuberculosis* protein tyrosine phosphatase B inhibitors, *Bioorganic & Medicinal Chemistry Letters* (2018), doi: <https://doi.org/10.1016/j.bmcl.2018.12.009>

This is a PDF file of an unedited manuscript that has been accepted for publication. As a service to our customers we are providing this early version of the manuscript. The manuscript will undergo copyediting, typesetting, and review of the resulting proof before it is published in its final form. Please note that during the production process errors may be discovered which could affect the content, and all legal disclaimers that apply to the journal pertain.



**Synthesis, biological evaluation and molecular docking study of 1,2,3-1*H*-triazoles having 4*H*-pyrano[2,3-*d*]pyrimidine as potential *Mycobacterium tuberculosis* protein tyrosine phosphatase B inhibitors**

Nguyen Dinh Thanh <sup>a\*</sup>, Do Son Hai <sup>a,b</sup>, Nguyen Thi Thu Ha <sup>a</sup>, Do Tien Tung <sup>a</sup>, Cao Thi Le <sup>a</sup>, Hoang Thi Kim Van <sup>a,c</sup>, Vu Ngoc Toan <sup>a,d</sup>, Duong Ngoc Toan <sup>a,e</sup>, Le Hai Dang <sup>a,f</sup>

<sup>a</sup> Faculty of Chemistry, VNU University of Science, 19 Le Thanh Tong, Ha Noi, Viet Nam

<sup>b</sup> Institute of Technique in Chemistry, Biology and Security Documents (Ministry of Public Security), Cau Giay, Ha Noi, Viet Nam

<sup>c</sup> Faculty of Chemical Technology, Viet Tri University of Industry, Tien Kien, Lam Thao, Phu Tho, Viet Nam

<sup>d</sup> Institute for Chemistry and Materials, Military Institute of Science and Technology (Ministry of Military), Cau Giay, Ha Noi, Viet Nam

<sup>e</sup> Faculty of Chemistry, Thai Nguyen University of Education, 20 Luong Ngoc Quyen, Thai Nguyen, Viet Nam

<sup>f</sup> Thai Nguyen College of Education, Quang Trung, Thinh Dan, Thai Nguyen, Viet Nam

### **Abstracts**

Some heterocycles, namely 2-amino-4*H*-pyran-3-carbonitriles, were synthesized in a three-component reaction from substituted benzaldehydes, malononitrile, and ethyl acetoacetate. These heterocycles have been converted subsequently into 4*H*-pyrano[2,3-*d*]pyrimidine ring by ring-closing reaction with acetic anhydride in the presence of the concentrated sulfuric acid as catalyst. The successive alkylation reaction of lactam N–H bond on pyrimidine-4-one ring was carried out using propargylic bromide in dry acetone in the presence of anhydrous potassium carbonate. The click chemistry of 3-propargyl-4*H*-pyrano[2,3-*d*]pyrimidine compounds has been accomplished by reaction with tetra-*O*-acetyl- $\alpha$ -D-

glucopyranosyl azide using the metal-organic framework Cu@MOF-5 as a catalyst in absolute ethanol. All the synthesized 1*H*-1,2,3-triazoles **8a-y** were screened for their *in vitro* *Mycobacterium tuberculosis* protein tyrosine phosphatase B (MtbPtpB) inhibition. Kinetic studies of the most active compounds **8v**, **8x**, and **8y** showed their competitive inhibition toward the MtbPtpB enzyme. The detailed structure-activity relationship (SAR) *in vitro* and *in silico* studies suggested that the interaction of Arg63 amino acids with anion type of *para*-hydroxyl group *via* a salt bridge of iminium cation was essential for strong inhibitory activity against MtbPtpB.

### Keywords

2-Amino-4*H*-pyran-3-carbonitriles; Antitubercular activity; Molecular docking; 4*H*-Pyrano[2,3-*d*]pyrimidine; PtpB.

It's known that *Mycobacteria* were bacteria, which caused serious diseases in human and animals. These bacteria included tuberculosis (*M. tuberculosis*) and the classic Hansen's strain of leprosy (*Mycobacterium leprae*). Among these bacteria, *Mycobacterium tuberculosis* caused tuberculosis due to the lack of proper therapeutic agents for its remedy.<sup>1</sup> The morbidity and mortality from tuberculosis and the emergence of multidrug-resistant (MDR) strains of *M. tuberculosis* became growing health problems in the world, particularly in Vietnam.<sup>2, 3</sup> Nowadays, Viet Nam is a lower, middle income country and is one of the 30 highest TB burden countries.<sup>4</sup> Tuberculosis (TB) kills nearly 2 million people annually in the world. The World Health Organization (WHO) declared that TB is as a global health emergency, which highlights the importance of TB as a major threat to humans.<sup>4</sup> The actions of second-line antituberculosis drugs were applied as the last resort for combating MDR infections when the first-line protocols were no effective in tuberculosis cases due to resistance problems.<sup>3</sup> On the other hand, drug resistance and patient noncompliance are two key factors that affect the success rate of

conventional treatments against TB. Therefore, there is an urgent need to identify novel therapeutic targets for TB treatment as well as new drugs that could act on them. Tuberculosis infections by drug-sensitive strains could be successfully treated using the specific remedy, but the appearance of drug-resistant strains of *M. tuberculosis* have promoted researches in new drug development, particularly the search for new drug targets. Protein tyrosine phosphatases (PTPs) are an important class of enzymes. Together with protein tyrosine kinases (PTKs), they control the level of phosphorylation of their protein substrate targets. Protein tyrosine phosphorylation plays a critical role in the signal transduction of many cellular events including immune response, metabolism, growth and gene transcription.<sup>5, 6</sup> It is known that there are two protein tyrosine phosphatases (PtpA and PtpB) secreted by MTB in infected human macrophages.<sup>7</sup> These enzymes have been recognized in MTB's genome.<sup>8</sup> One assumed that these enzymes are profitable targets for the development of novel therapeutics against TB.<sup>9, 10</sup> Although several reports realize that PtpA and PtpB inhibition by small molecules could affect MTB survival in the host, thus paving the way for the development of innovative therapeutic strategies.<sup>10-12</sup>

Recently, the syntheses of pyranopyrimidine derivatives have obtained interest in medicinal chemistry due to the broad range of their pharmacological activities. Pyrano[2,3-*d*]pyrimidine is an unsaturated heterocyclic system which is formed by fusion of two six member pyran and pyrimidine rings together. This ring system consisted of one oxygen atom at position 8 and two nitrogen atoms at positions 1 and 3, respectively. It is realized that if pyrano[2,3-*d*]pyrimidine moiety are connected to one certain molecule, then resultant derivative can enhance its inherent pharmaceutical activity in bioactive compounds, such as antitumour,<sup>13</sup> antitubercular,<sup>14</sup> antibacterial,<sup>15, 16</sup> antifungal,<sup>16</sup> antimicrobial<sup>17</sup> activities, and so on. Figure 1 below represented some bioactive compounds. Kamdar *et al.* showed that compound **A**, which was fused with quinoline ring, had antitubercular activity against *M. tuberculosis* with MIC = 62.5 µg/mL.<sup>14</sup> Sabry *et al.* indicated that benzopyrano[2,3-*d*]pyrimidines **B** with chloro- and bromo-substituents had inhibitory activities against some typical Gram-negative (and) Gram-positive bacteria, and fungi with MICs = 14–27, 15–26, and 15–24 µg/mL, respectively.<sup>18</sup> According

to Dangolani *et al.*, compound **C** had antioxidant activity as Trolox equivalent antioxidant capacity (TEAC) with  $TEAC = 5.237 \pm 0.053 \mu M$ .<sup>19</sup> Paliwal *et al.* announced that compounds **D** had good anticancer and antibacterial activities.<sup>20</sup> Kalaria and co-workers showed that fused pyran derivative **E** had antimalarial activity with  $IC_{50}$  of  $0.062 \mu g/mL$  and 92% inhibition against *M. tuberculosis* H<sub>37</sub>Rv at concentration of  $100 \mu g/mL$ .<sup>21</sup>

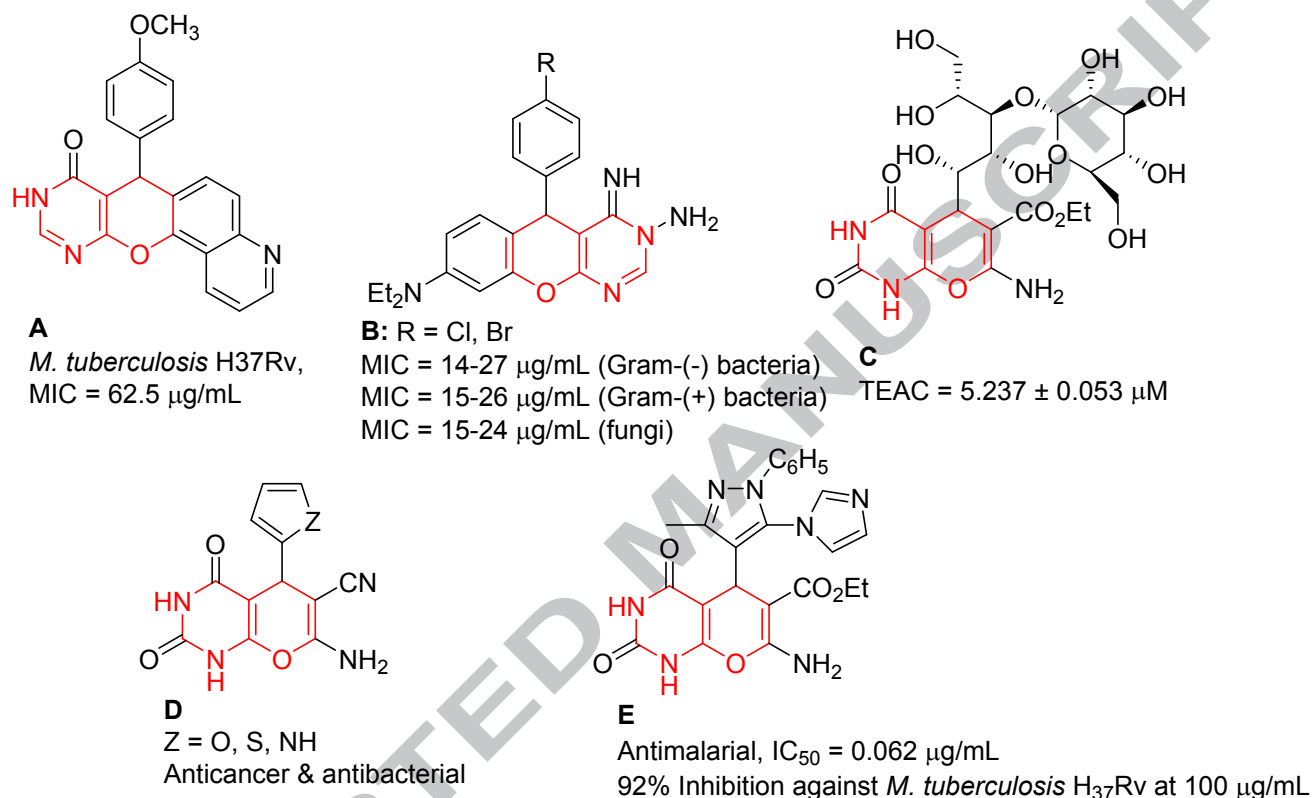


**Figure 1.** Some pyrano[2,3-*d*]pyrimidine derivatives having biological activities.

Besides derivatives containing pyrano[2,3-*d*]pyrimidine ring, 1*H*-1,2,3-triazoles are also studied for their biological, therapeutic and industrial potential.<sup>22, 23</sup> 1*H*-1,2,3-Triazoles set up an important class of nitrogen-containing heterocycles in the area of organic and medicinal chemistry. Medicinally, they showed a broad range of diverse interesting pharmacological properties such as antitubercular,<sup>24</sup> anticancer,<sup>25</sup> anti-HIV,<sup>26</sup> antiallergic,<sup>27</sup> antimalarial,<sup>28</sup> antifungal,<sup>29</sup> and antibacterial<sup>30</sup> activities, and so on. Some 1*H*-1,2,3-triazoles were potential MtbPtpB inhibitors, such as compound **F** with significant cellular activity ( $IC_{50} 1.27 \mu M$ );<sup>31</sup> 1,2,3-1*H*-triazole **G** was the most active representative in the library

of MTB PtpB inhibitors,<sup>32</sup> with a  $K_i$  value of 0.15  $\mu\text{M}$  and  $\text{IC}_{50} = 0.64 \mu\text{M}$  (Fig. 2). Some nucleosides and oligonucleotides bearing 1*H*-1,2,3-triazole residues with nucleobase have been synthesized and studied for antitumor,<sup>25</sup> antiviral<sup>33</sup> and antitubercular<sup>34</sup> activities, as 1*H*-1,2,3-triazole **H** bearing D-galactose inhibited bacterial growth by 76% and 78% at concentrations of 5  $\mu\text{g/mL}$  and 25  $\mu\text{g/mL}$ , respectively (Fig. 2).<sup>35</sup>

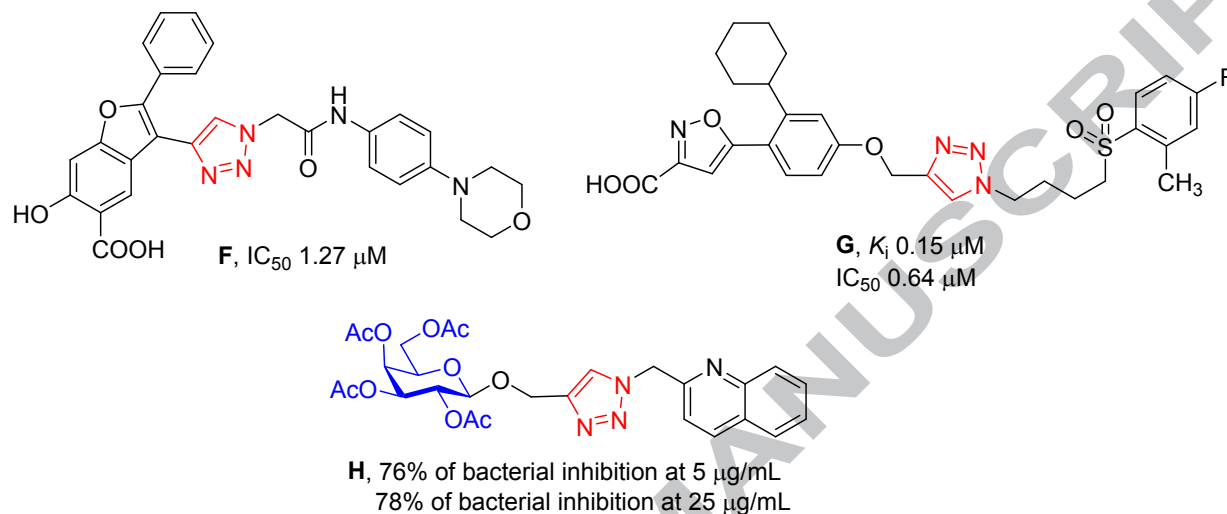


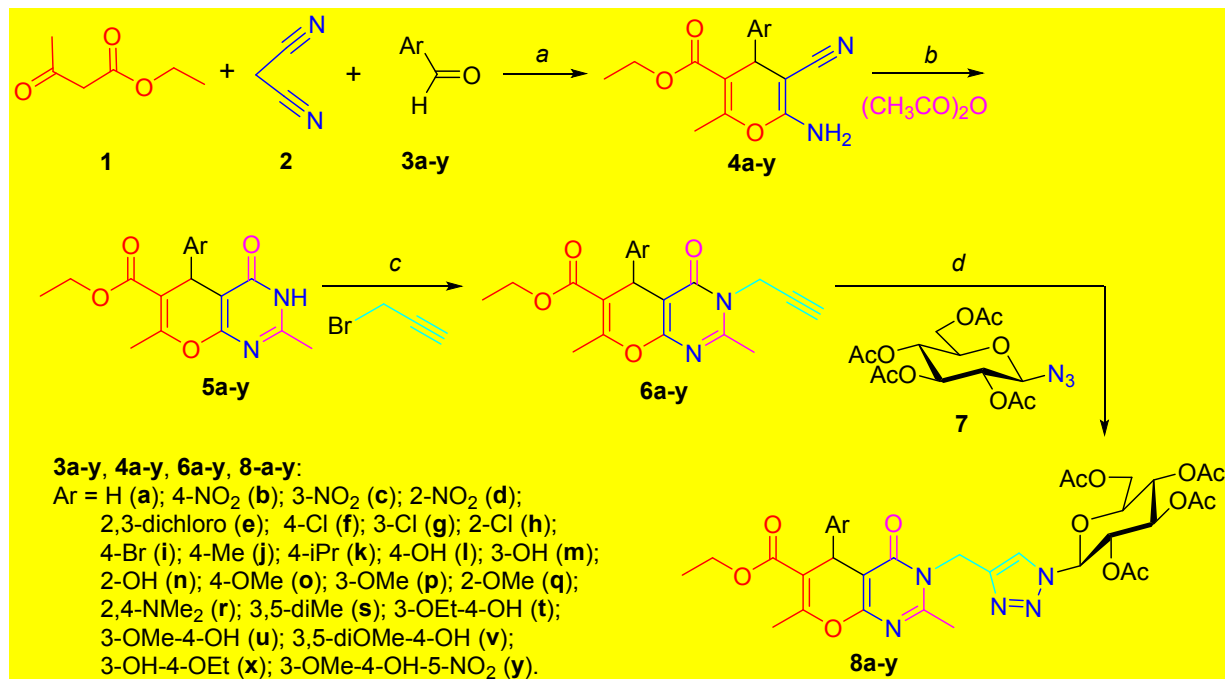
**Figure 2.** Some structures of selected MtbPtpB inhibitors having 1*H*-1,2,3-triazole ring.

The connection of these above pharmacophores could bring forth remarkably biological activities or strengthen their inherent biological activities in new derivatives. They helped to find the bioactive compounds easily and favorably. On the other hand, pyrano[2,3-*d*]pyrimidine system have been synthesized directly by the reaction of aromatic aldehydes, malononitrile or cyanoacetic ester or chalcones (arylideneacetophenones) with barbituric acid under different catalytic conditions, such as microwave irradiations, ultrasonic irradiations, solvent free condition and in aqueous medium in the absence of catalysts.<sup>36, 37</sup> In addition, this ring could be synthesized from 2-amino-4*H*-pyran-3-carbonitriles by taking advantage of the chemistry of amino and nitrile groups.<sup>38</sup> Up to now, the connection between 4*H*-pyrano[2,3-*d*]pyrimidine and D-glucose ring tethering by 1*H*-1,2,3-triazole was not touched upon. Therefore, we have designed molecules that contained both pyrano[2,3-*d*]pyrimidine and 1*H*-1,2,3-triazole ring having D-glucose moiety. We reported herein the synthesis of substituted

4*H*-pyrano[2,3-*d*]pyrimidines bearing propargyl unit and its click chemistry. We further evaluated the *in vitro* inhibitory activity of synthesized 1*H*-1,2,3-triazole-tethered 4*H*-pyrano[2,3-*d*]pyrimidines and D-glucose conjugates against *M. tuberculosis* protein tyrosine phosphatase PtpB.

The 4*H*-pyrano[2,3-*d*]pyrimidines **5a-y** were synthesized from corresponding ethyl 6-amino-5-cyano-2-methyl-4-aryl-4*H*-pyran-3-carboxylates **4a-y** by cyclizing with acetic anhydride (and) using concentrated sulfuric acid as catalyst. The yields of these products were 62–71% (Scheme 1). In turn, ethyl 4*H*-pyran-3-carboxylates **4a-y** were prepared by three-component reaction between ethyl acetoacetate **1**, malononitrile **2** and substituted benzaldehydes **3a-y** in 63–89% yields. Ammonium hydroxide (Ammonium solution 25%) or Cu@MOF-5 were used as the catalysts in these reactions. In general, the latter gave higher yields of **4a-y** (63–89% in method A *v.s.* 78–90% in method B).

Ring-closing reaction with acetic anhydride of 4*H*-pyrans **4a-y** into the corresponding 4*H*-pyrano[2,3-*d*]pyrimidines **5a-y** was confirmed by IR and NMR spectra. The ring-closing process was confirmed by the disappearance of the amino group, with two IR absorption bands in the regions at 3420–3250 cm<sup>-1</sup>, and by the appearance of IR absorption band of the amido group of the pyrimidine-4-one ring in the region at 1672–1643 cm<sup>-1</sup>. The signal of the 2H integral of an amino group in  $\delta = 7.09\text{--}6.86$  ppm also was no longer present, and simultaneously a signal singlet with 1H integral appeared in extreme downfield region, with  $\delta=12.49\text{--}12.47$  ppm. The signal of proton H-5 of pyran ring also shifted toward downfield, at  $\delta=4.79\text{--}4.72$  ppm when compared with corresponding values of  $\delta=4.5\text{--}4.20$  ppm in the initial 4*H*-pyran **4a-y**. Three new signals appeared <sup>13</sup>C NMR spectra of these 4*H*-pyrano[2,3-*d*]pyrimidines, belong to the newly carbon atoms that were added to the molecular skeleton. That's carbon atom C-2, with  $\delta=160.4\text{--}160.3$  ppm, methyl group on position 2, with  $\delta=21.4\text{--}21.5$  ppm, and amide carbonyl carbon atom at  $\delta=162.4$  ppm, derived from the C≡N functional group (with NMR signal at  $\delta=120.3\text{--}119.8$  ppm, and no longer appeared in the <sup>13</sup>C NMR spectra of **5a-y**).



**Scheme 1.** Reagents and conditions: (a) Ammonium solution 25%, 25°C, 3 hrs., or Cu@MOF-5 (10 mol%), 96% EtOH, 50°C, 1 hr; (b) Acetic anhydride, conc. H<sub>2</sub>SO<sub>4</sub> (cat.), 15 min, in refluxing, then 25°C, 24 hrs.; (c) Propargyl bromide, anhydrous potassium carbonate, dry acetone, in refluxing, 4–5 hrs; (d) Cu@MOF-5 (cat.), 79–80°C, abs. EtOH, 4–5 hrs.

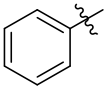
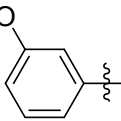
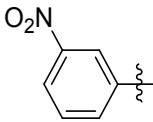
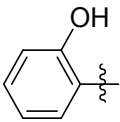
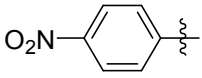
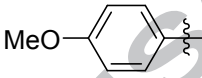
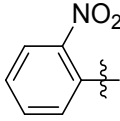
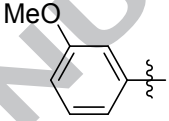
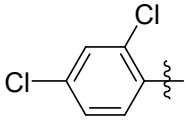
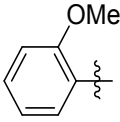
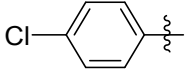
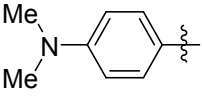
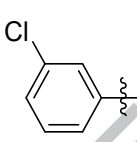
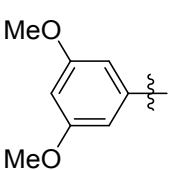
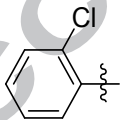
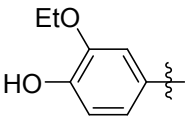
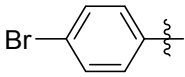
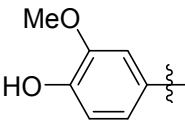
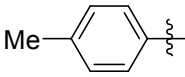
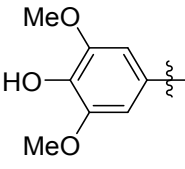
Reaction of 4*H*-pyrano[2,3-*d*]pyrimidines **5a-y** with propargyl bromide in dry acetone in the presence of anhydrous K<sub>2</sub>CO<sub>3</sub> gave corresponding *N*-propargyl derivatives **6a-y** with the yields of 76–88%. The *N*-propargylation reaction of the lactam group of pyrimidine ring was confirmed by the appearance of two proton signals of the CH<sub>2</sub> group, of the terminal alkyne in <sup>1</sup>H NMR spectra, and of three carbon-13 signals in the <sup>13</sup>C NMR spectra of the propargyl group, –CH<sub>2</sub>C≡CH. The two protons of the propargyl-methylene group were not equivalent to each other in the magnetic term. Therefore, their signals split due to spin-spin coupling in the doublet-doublet signal with vicinal coupling constant *J*=18.0 Hz. There is another interaction with the acetylenic proton in faraway with coupling constant *J*=2.5 Hz. However, due to the small coupling constants, the signal of this acetylenic proton degenerate into counterfeit

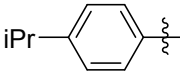
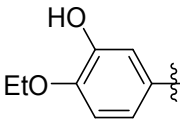
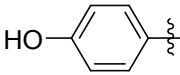
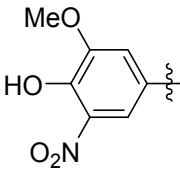
singlet in  $\delta=3.50\text{--}3.35$  ppm. On the other hand, the absence of NH signal in extreme downfield region ( $\delta=12.49\text{--}12.47$  ppm) also denoted that the propargyl group was attached to the N–H bond.

Click chemistry of *N*-propargyl derivatives **6a–y** of 4*H*-pyrano[2,3-*d*]pyrimidines with 2,3,4,6-tetra-*O*-acetyl- $\beta$ -D-glucopyranosyl azide **7** gave corresponding 1*H*-1,2,3-triazoles **8a–y** with the yields of 64–94%. The processes were catalyzed by Cu@MOF-5. The reaction solvent was absolute ethanol for 4–5 hrs. IR spectra of **8a–y** had strong absorption bands in the regions of 1757–1747, 1236–1224, and 1041–1037  $\text{cm}^{-1}$  belonging to C=O acetyl stretching vibrations of acetate group in peracetylated D-glucose moiety. The  $^{13}\text{C}$  resonance signals of these group had two regions, with  $\delta = 170.50\text{--}168.90$  ppm belonging to C=O acetate ester group and  $\delta = 20.98\text{--}20.27$  ppm belonging to a methyl-acetate group. Chemical shifts of protons in D-glucose moiety were in the range of  $\delta = 6.38\text{--}4.08$  ppm. The carbon atoms of the D-glucopyranose ring had six resonance signals at  $\delta = 84.3\text{--}62.2$  ppm. The coupling constants between protons H-2 and H-3 were  $J = 9.50\text{--}9.25$  Hz that indicated the  $\beta$ -anomeric configuration of this glucoside. The 1*H*-1,2,3-triazole ring (was) specified by the unique proton of the 1*H*-1,2,3-triazole ring that had a downfield chemical shift at  $\delta = 8.55\text{--}8.54$  ppm in a singlet. This signal could be used to identify the formation of the 1*H*-1,2,3-triazole system. Two C-a and C-b carbon atoms of this ring had  $^{13}\text{C}$  NMR signals in the regions at  $\delta = 123.4\text{--}123.3$  ppm and  $\delta = 143.2\text{--}142.9$  ppm, respectively. The two protons of the  $\text{CH}_2\text{O}$  bridged group between the 1,2,3-triazole ring and chromene ring were not magnetically equivalent, so their signal was located in the regions at  $\delta = 5.34\text{--}5.25$  and  $5.07\text{--}5.01$  ppm. Carbon atom of this bridged group had a chemical shift at  $\delta = 40.1\text{--}39.9$  ppm, and this signal shifted more downfield due to the electronegative influence of oxygen atom and the anisotropic effect of triazole ring.

All the synthesized compounds **8a–y** were screened for their *in vitro* MtbPtpB inhibition. MtbPtpB is a virulence factor from *Mycobacterium tuberculosis*, which was cloned, expressed, and purified as recently described.<sup>7</sup>  $\text{IC}_{50}$  values were the average of three independent experiments. The obtained results are shown in Table 1.

**Table 1.** IC<sub>50</sub> values of are shown for MtbPtpB<sup>a</sup>

| Compd.    | Phenyl ring   | IC <sub>50</sub> , μM | Compd.    | Phenyl ring  | IC <sub>50</sub> , μM |
|-----------|---|-----------------------|-----------|--|-----------------------|
| <b>8a</b> |    | 47.03±1.81            | <b>8m</b> |    | 35.95±2.29            |
| <b>8b</b> |    | 45.01±2.32            | <b>8n</b> |    | 28.96±3.13            |
| <b>8c</b> |    | 33.03±2.53            | <b>8o</b> |    | 29.02±3.14            |
| <b>8d</b> |    | 35.13±2.24            | <b>8p</b> |    | 28.24±2.63            |
| <b>8e</b> |   | 44.02±2.53            | <b>8q</b> |   | 35.04±2.61            |
| <b>8f</b> |  | 35.3±2.2              | <b>8r</b> |  | 32.04±2.11            |
| <b>8g</b> |  | 9.52±1.13             | <b>8s</b> |  | 32.51±2.13            |
| <b>8h</b> |  | 33.21±3.32            | <b>8t</b> |  | 7.94±0.23             |
| <b>8i</b> |  | n.a.                  | <b>8u</b> |  | 7.51±0.33             |
| <b>8j</b> |  | n.a.                  | <b>8v</b> |  | <b>2.22±0.23</b>      |

| Compd.    | Phenyl ring   | IC <sub>50</sub> , μM | Compd.    | Phenyl ring  | IC <sub>50</sub> , μM |
|-----------|---|-----------------------|-----------|--|-----------------------|
| <b>8k</b> |  | n.a.                  | <b>8x</b> |  | <b>3.53±0.19</b>      |
| <b>8l</b> |  | 35.34±3.10            | <b>8y</b> |  | <b>1.56±0.21</b>      |

n.a = not active (no inhibition up to a concentration of 100 μM).

<sup>a</sup> All IC<sub>50</sub> values were calculated from at least three independent measurements.

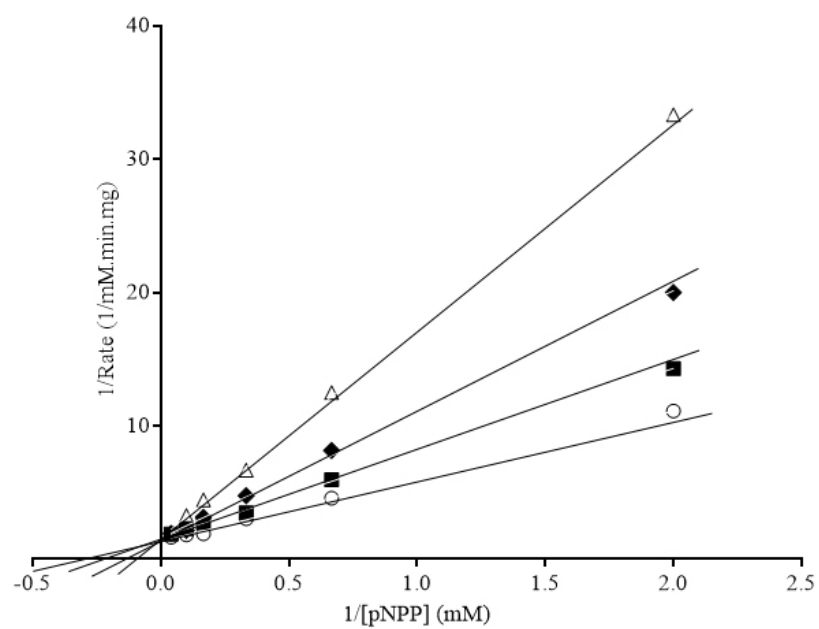
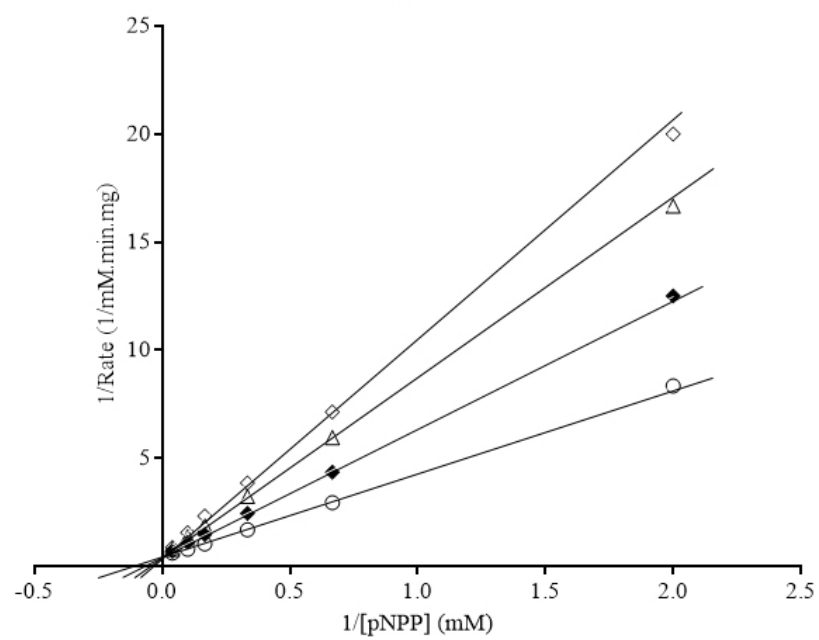
Amongst twenty-four screened compounds, six 1*H*-1,2,3-triazoles **8g**, **8t**, **8u**, **8v**, **8x**, and **8y** displayed inhibitory activity against MtbPtpB with IC<sub>50</sub> ranging from 1.56 to 9.52 μM (Table 1). The remaining compounds with IC<sub>50</sub> values >100 μM did not exhibit inhibitory activity. Among the above mentioned active compounds, the compounds having more potent inhibitory activity against MtbPtpB (with IC<sub>50</sub> values <5 μM), **8v**, **8x**, and **8y**, had a hydroxyl group on *para*-position and methoxy, ethyl groups on *meta*-position of the benzene ring. The IC<sub>50</sub> values of these compounds were 2.22, 3.53, and 1.56 μM, respectively. The 1*H*-1,2,3-triazoles **8v** and **8y** had the highest inhibitory activity against MtbPtpB. In these cases, the presence of the second substituent in *meta*-position helped to increase the activity (methoxy or nitro groups). Especially, the presence of nitro on *meta*-position in **8y** (IC<sub>50</sub> = 1.56 μM) enhanced significantly the inhibitory activity against MtbPtpB of this compound compared to compound **8v** (IC<sub>50</sub> = 2.22 μM), whereas the methoxy or nitro substituents located (at) the *ortho*- or *para*-positions made the inhibitory activity decreasing. The situation happened in 1*H*-1,2,3-triazoles **8d** (IC<sub>50</sub> = 35.13 μM) and **8q** (IC<sub>50</sub> = 35.04 μM). The absence of the hydroxyl group in *para*-position in compound **8s** also reduced the inhibitory activity (its IC<sub>50</sub> value of 32.51 μM).

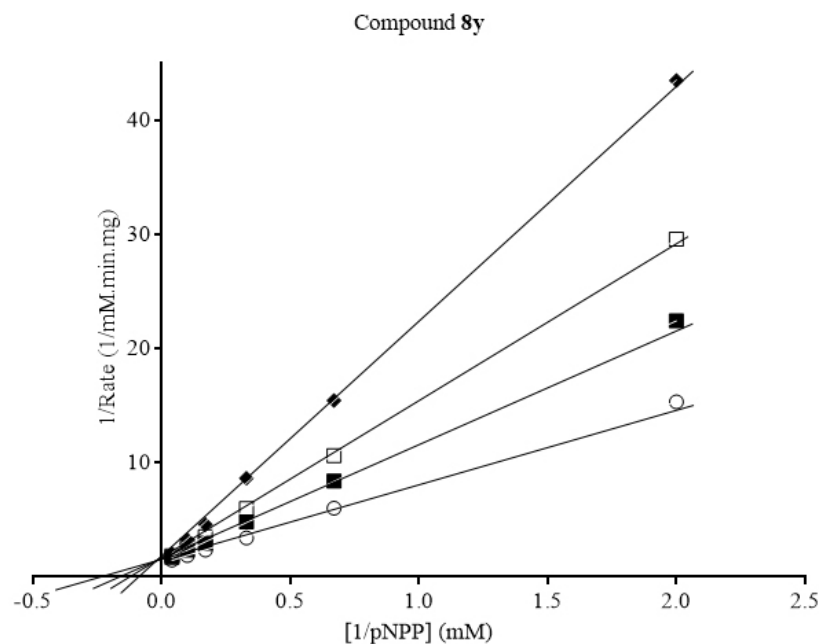
*Determination of the mode of inhibition of MtbPtpB by the identified inhibitors*

The type of inhibition with respect to the substrate *p*-nitrophenyl phosphate (*p*NPP) was determined for the most active compounds (inhibitors) **8x**, **8y**, and **8v**. The obtained kinetic measurements showed that the inhibitors exhibited degrees of saturation and release of *p*-nitrophenol following a classic Michaelis-Menten enzymatic mechanism.<sup>39, 40</sup> For compounds **8x**, **8y**, and **8v**, all lines converged at the *y*-axis ( $1/V_{\max}$ ) in Lineweaver-Burk double-reciprocal plots (Fig. 3), and the slope ( $K_{\text{Mapp}}/V_{\max}$ ) and *x*-axis interception ( $-1/K_{\text{Mapp}}$ ) according to the inhibitor concentrations. The inhibition constants  $K_i$  obtained for **8x**, **8y**, and **8v** were of 2.16, 1.10, and 1.80  $\mu\text{M}$ , respectively (Table 2). Therefore, the constant value of  $V_{\max}$  and the increased values of  $K_{\text{Mapp}}$  are consistent with a competitive inhibition mechanism of the evaluated compounds.<sup>39</sup>

**Table 2.**  $K_i$  values,  $\text{IC}_{50}/K_i$  ratio and type of inhibition of the MtbPtpB inhibitors.

| Compd.    | $K_i$ ( $\mu\text{M}$ ) | $\text{IC}_{50}$ ( $\mu\text{M}$ ) | $\text{IC}_{50}/K_i$ | Type of inhibition |
|-----------|-------------------------|------------------------------------|----------------------|--------------------|
| <b>8v</b> | $1.80 \pm 0.07$         | $2.22 \pm 0.23$                    | 1.23                 | Competitive        |
| <b>8x</b> | $2.16 \pm 0.14$         | $3.53 \pm 0.19$                    | 1.63                 | Competitive        |
| <b>8y</b> | $1.10 \pm 0.09$         | $1.56 \pm 0.21$                    | 1.42                 | Competitive        |

Compound **8v**Compound **8x**

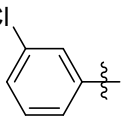
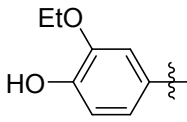
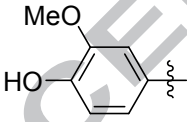
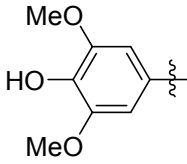
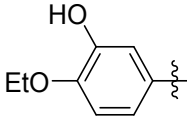
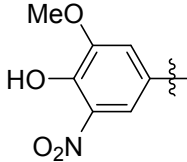


**Figure 3.** Competitive inhibitory profile of the most active compounds **8v**, **8x**, and **8y**. Lineweaver-Burk double-reciprocal plots represented inhibitory profiles of these compounds against MtbPtpB. Kinetic experiments were conducted in the presence of increasing concentrations of inhibitors: 0  $\mu\text{M}$  ( $\circ$ ), 1  $\mu\text{M}$  ( $\blacksquare$ ), 1.5  $\mu\text{M}$  ( $\square$ ), 2  $\mu\text{M}$  ( $\blacklozenge$ ), 3  $\mu\text{M}$  ( $\triangle$ ), 4  $\mu\text{M}$  ( $\diamond$ ); *p*NPP was used as substrate in all experiments.

Based on the results obtained from the enzymatic assays, molecular modeling studies were performed as a step toward understanding the interaction mode of these compounds as inhibitors. We examined the docking of (the) highest inhibitory activity compounds **8v**, **8x**, and **8y**. Simultaneously, compounds more active **8g**, **8t**, and **8u**, which had  $\text{IC}_{50} < 10 \mu\text{M}$ , were also considered in the molecular docking study. Crystal structure of *M. tuberculosis* protein tyrosine phosphatase MtbPtpB, was retrieved from the RCSB Protein Data Bank (<https://www.rcsb.org/structure/2oz5>), in complex with the specific inhibitor OMTS (PDB code: 2OZ5).<sup>41</sup> The favorably docked molecules were ranked according to the XP Glide Score (Table 3). Compound **8y** gave a better glide score when compared with other five compounds for the target protein, with binding score of  $-12.215 \text{ kcal/mol}$ . The important intermolecular protein-ligand interactions of compound **8y** are depicted in Figure 4, and the ones of the

remaining compounds were represented in the figures in Section 6 (in [Supplementary Data](#) in online version of this article). There were intermolecular amino acid interactions with compounds **8g**, **8t**, **8u**, **8v**, **8x**, and **8y**. The ligand-amino acid interaction of residue Ser57 always took place in all the ligands. Both Ser57 and Hid94 had hydrogen-bonding interactions with C=O acetate of D-glucose moiety on positions 6 and 4, respectively. Residue Phe98 always had  $\pi$ - $\pi$  interactions with 4*H*-pyrano[2,3-*d*]pyrimidine ring of all the ligands. This suggested that  $\pi$ - $\pi$  interaction improved the docking scores. In ligands **8t**, **8u** and **8v**, there was a supplemental  $\pi$ - $\pi$  interaction of this residue to the benzene ring. However, this one may seem unimportant in interactions with enzyme because docking score in these cases decreased insignificantly.

**Table 2.** Molecular docking analysis of protein target 2OZ5 with selected compounds **8g**, **8t**, **8u**, **8v**, **8x**, and **8y**

| Compd.    | Phenyl ring   | Glide score*   | IC <sub>50</sub> (μM) | Compd.    | Phenyl ring   | Glide score*   | IC <sub>50</sub> (μM) |
|-----------|---|----------------|-----------------------|-----------|---|----------------|-----------------------|
| <b>8g</b> |  | -9.881         | 9.52±1.13             | <b>8t</b> |  | -10.220        | 7.94±0.23             |
| <b>8u</b> |  | -10.006        | 7.51±0.33             | <b>8v</b> |  | <b>-10.435</b> | <b>2.22±0.23</b>      |
| <b>8x</b> |  | <b>-10.337</b> | <b>3.53±0.19</b>      | <b>8y</b> |  | <b>-12.215</b> | <b>1.56±0.21</b>      |

\* In kcal/mol.

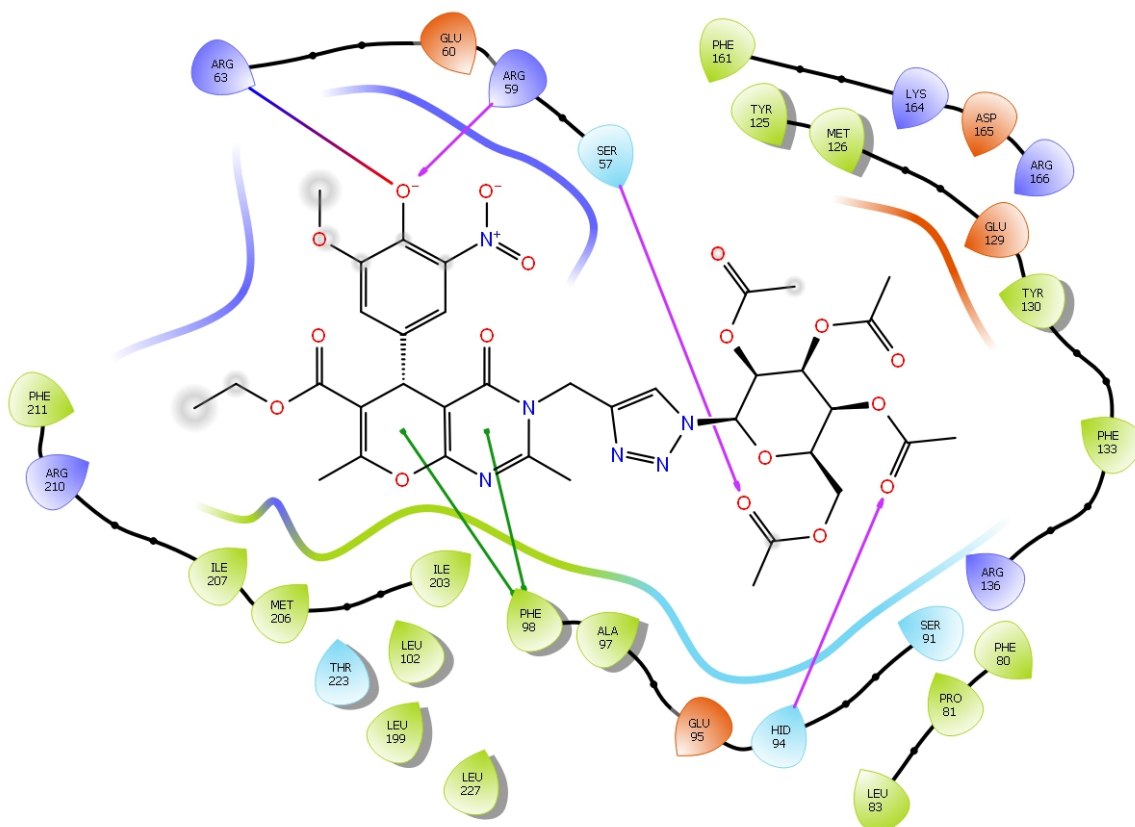
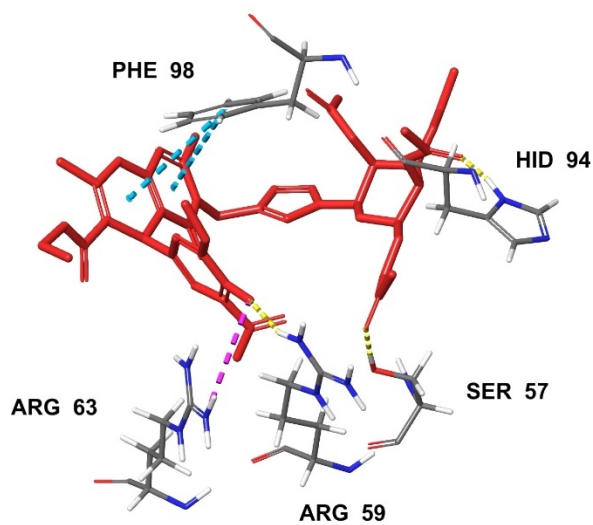
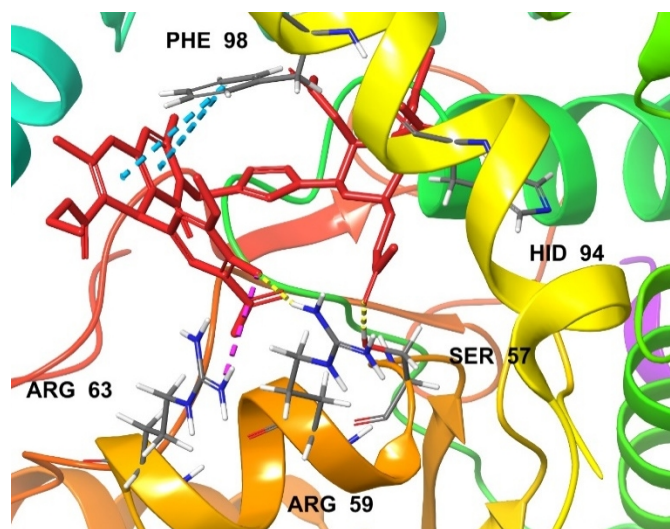


**Figure 4.** Amino acids involved in intermolecular interactions of 1*H*-1,2,3-triazole **8y**.

(a)



(b)



o(c)

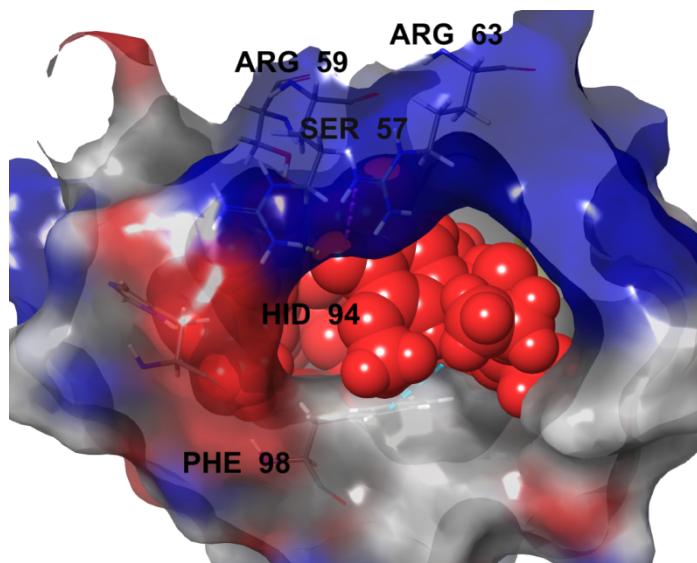


**Figure 5.** (a,b) Compound **8y** (in red color) in MTB phosphotyrosine phosphatase B protein (PDB ID: 2OZ5). (c) Alignment of compound **8y** in the binding pocket (in residue-charge color scheme).

There was a  $\pi$ -cation interaction (electrostatic interaction) *via* imine group between residue Arg166 and 1*H*-1,2,3-triazole ring in case of compound **8v**. This diminished its docking score ( $-10.435$  kcal/mol). Residues Ser57, Arg59, Arg63, and Hid94 interacted with compound **8y** showing high ligand exposure. Phe98 had two  $\pi$ - $\pi$  interactions with the compound **8y**, one with pyran ring, and another with pyrimidine ring. Residue Arg63 interacted electrostatically with anion type of *para*-hydroxyl group *via* a salt bridge of iminium cation and Arg59 interacted with this anion *via* hydrogen-bonding interaction. This resulted in compound **8y** showing the highest binding energy values of  $-12.215$  kcal/mol. The electrostatic interaction in compounds **8v** and **8y** also perfected the docking scores. Compound **8y** is bound to the active site amino acid residues in the pocket region as shown in Figure 5a,b. The pocket region of 2OZ5 is present in a loop region encompassed by alpha helix chains seen in Figure 5b (**8y** in red color). The location and orientation of the triazole group were complementary to the surrounding MtbPtpB side chains, which created a specific binding pocket. These observations indicated that compound **8y** could have an important role in anchoring within the active site of the receptor.

In summary, a series of novel 4*H*-pyrano[2,3-*d*]pyrimidine bearing D-glucose moiety tethered 1,2,3-triazole derivatives were synthesized *via* an easy and convenient synthetic protocol starting from substituted benzaldehydes, ethyl acetoacetate, and malononitrile. The synthesis of 24 analogs **8a-y** accomplished in four-step sequences using click chemistry in the key step. Their structures were fully characterized by IR, NMR and mass spectral data. The *in vitro* inhibition evaluation on MtbPtpB study of all the compounds revealed six compounds found to be active against *M. tuberculosis* PtpB. Amongst six 1*H*-1,2,3-triazoles **8g**, **8t**, **8u**, **8v**, **8x**, and **8y** displayed inhibitory activity against MtbPtpB with IC<sub>50</sub> ranging from 1.56 to 9.52 μM, compound **8y** is the most potent compound *in vitro* with an IC<sub>50</sub> value of 1.56 μM. Kinetic studies of the most active compounds **8v**, **8x**, and **8y** showed the competitive inhibition of toward the MtbPtpB enzyme. Cross-docking studies revealed compound **8y** to be more effective against *Mycobacterium tuberculosis* protein tyrosine phosphatase. Docking results indicated that Ser57, Arg59, Hid94, and Phe98 amino acids in the binding pocket as potential ligand binding hot-spot residues.

### Acknowledgements

This research is funded by Vietnam National Foundation for Science and Technology Development (NAFOSTED) under grant number 104.01-2017.02.

### Supplementary data

Supplementary data (experimental section, IR, <sup>1</sup>H NMR, <sup>13</sup>C NMR and ESI-Mass spectral data for the synthesized compounds), and also ligand-docking results associated with this article can be found, in the online version, at <http://dx.doi.org/10.1016/j.bmcl...>

## References

1. Dye C. Global epidemiology of tuberculosis. *Lancet*. 2006;367(9514):938–940.  
[https://doi.org/10.1016/S0140-6736\(06\)68384-0](https://doi.org/10.1016/S0140-6736(06)68384-0).
2. Beyer P, Moorthy V, Paulin S, et al. The drugs don't work: WHO's role in advancing new antibiotics. *Lancet*. 2018;392(10144):264–266. [https://doi.org/10.1016/S0140-6736\(18\)31570-8](https://doi.org/10.1016/S0140-6736(18)31570-8).
3. Zignol M, Dean AS, Falzon D, et al. Twenty Years of Global Surveillance of Antituberculosis-Drug Resistance. *New Eng J Med*. 2016;375(11):1081–1089.  
<https://doi.org/10.1056/NEJMSr1512438>.
4. WHO. Global tuberculosis report 2017. 2017.  
[http://www.who.int/tb/publications/global\\_report/en/](http://www.who.int/tb/publications/global_report/en/).
5. Bialy L, Waldmann H. Inhibitors of Protein Tyrosine Phosphatases: Next-Generation Drugs? *Angew Chem Int Ed*. 2005;44(25):3814–3839. <https://doi.org/10.1002/anie.200461517>.
6. Lim WA, Pawson T. Phosphotyrosine Signaling: Evolving a New Cellular Communication System. *Cell*. 2010;142(5):661–667. <https://doi.org/10.1016/j.cell.2010.08.023>.
7. Koul A, Herget T, Klebl B, Ullrich A. Interplay between mycobacteria and host signalling pathways. *Nat Rev Microbiol*. 2004;2:189–202. <https://doi.org/10.1038/nrmicro840>.
8. Cole ST, Brosch R, Parkhill J, et al. Deciphering the biology of Mycobacterium tuberculosis from the complete genome sequence. *Nature*. 1998;393:537–544. <https://doi.org/10.1038/31159>.
9. Caselli A, Paoli P, Santi A, et al. Low molecular weight protein tyrosine phosphatase: Multifaceted functions of an evolutionarily conserved enzyme. *Biochim Biophys Acta Proteins Proteom*. 2016;1864(10):1339–1355. <https://doi.org/10.1016/j.bbapap.2016.07.001>.
10. Mascarello A, Chiaradia-Delatorre LD, Mori M, Terenzi H, Botta B. Mycobacterium tuberculosis-Secreted Tyrosine Phosphatases as Targets Against Tuberculosis: Exploring Natural Sources in Searching for New Drugs. *Curr Pharm Des*. 2016;22(12):1561–1569.  
<http://dx.doi.org/10.2174/1381612822666160112130539>.

11. Dutta NK, He R, Pinn ML, et al. Mycobacterial Protein Tyrosine Phosphatases A and B Inhibitors Augment the Bactericidal Activity of the Standard Anti-tuberculosis Regimen. *ACS Infect Dis*. 2016;2(3):231–239. <https://doi.org/10.1021/acsinfecdis.5b00133>.
12. Wong D, Bach H, Sun J, Hmama Z, Av-Gay Y. *Mycobacterium tuberculosis* protein tyrosine phosphatase (PtpA) excludes host vacuolar-H<sup>+</sup>-ATPase to inhibit phagosome acidification. *Proc Natl Acad Sci U S A*. 2011;108(48):19371–19376. <https://doi.org/10.1073/pnas.1109201108>.
13. Valderrama JA, Colonelli P, Vásquez D, González MF, Rodríguez JA, Theoduloz C. Studies on quinones. Part 44: Novel angucyclinone N-heterocyclic analogues endowed with antitumoral activity. *Biorg Med Chem*. 2008;16(24):10172–10181. <https://doi.org/10.1016/j.bmc.2008.10.064>.
14. Kamdar NR, Haveliwala DD, Mistry PT, Patel SK. Design, synthesis and in vitro evaluation of antitubercular and antimicrobial activity of some novel pyranopyrimidines. *Eur J Med Chem*. 2010;45(11):5056–5063. <https://doi.org/10.1016/j.ejmech.2010.08.014>.
15. Vekariya RH, Patel KD, Vekariya MK, et al. Synthesis of pyrazolo[4',3':5,6]pyrano[2,3-d]pyrimidine derivatives and their antimicrobial, antimalarial and antituberculosis evaluation. *Indian J. Chem*. 2018;57B:997–1005. <http://nopr.niscair.res.in/handle/123456789/44744>
16. Bhat AR, Shalla AH, Dongre RS. Microwave assisted one-pot catalyst free green synthesis of new methyl-7-amino-4-oxo-5-phenyl-2-thioxo-2,3,4,5-tetrahydro-1H-pyrano[2,3-d]pyrimidine-6-carboxylates as potent in vitro antibacterial and antifungal activity. *J Adv Res*. 2015;6(6):941–948. <https://doi.org/10.1016/j.jare.2014.10.007>.
17. Shamroukh AH, Zaki MEA, Morsy EMH, Abdel-Motti FM, Abdel-Megeid FME. Synthesis, Isomerization, and Antimicrobial Evaluation of Some Pyrazolopyranotriazolopyrimidine Derivatives. *Arch Pharm*. 2007;340(7):345–351. <https://doi.org/10.1002/ardp.200700007>.
18. Sabry NM, Mohamed HM, Khattab ESAEH, Motlaq SS, El-Agrody AM. Synthesis of 4H-chromene, coumarin, 12H-chromeno[2,3-d]pyrimidine derivatives and some of their antimicrobial

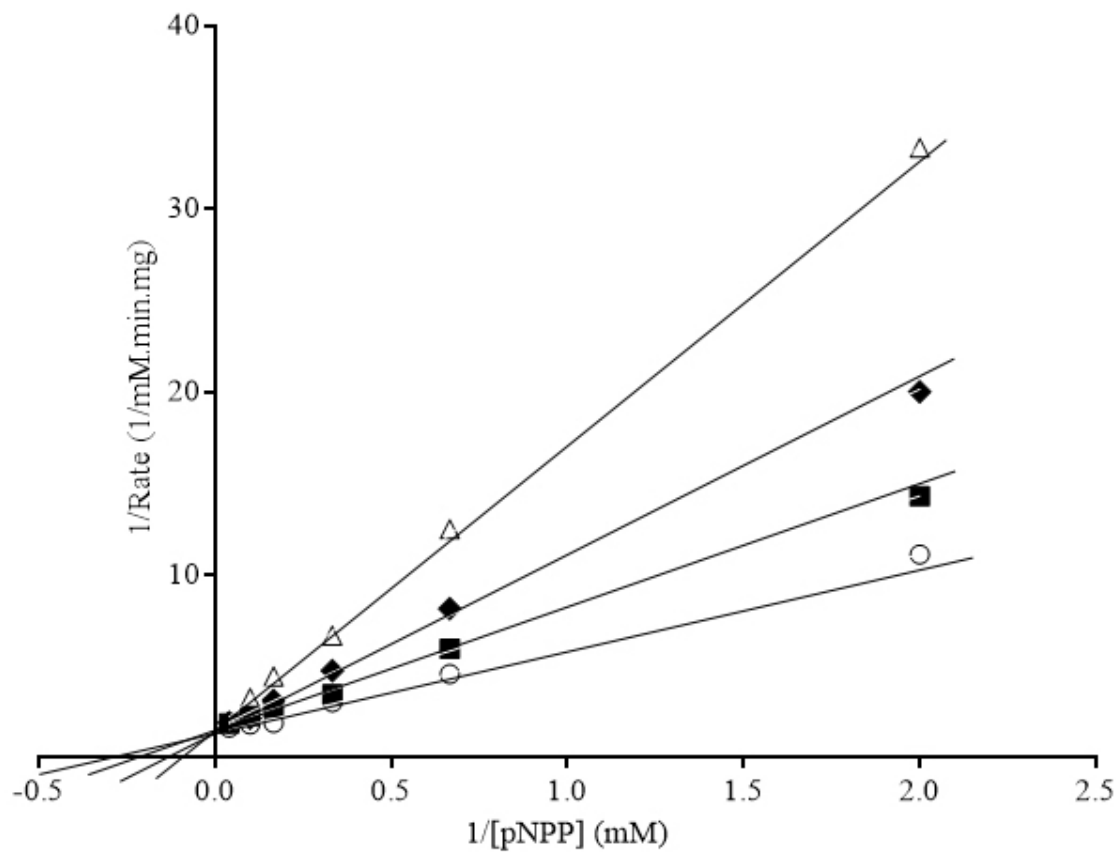
and cytotoxicity activities. *Eur J Med Chem.* 2011;46(2):765–772.

<https://doi.org/10.1016/j.ejmech.2010.12.015>.

19. Khajeh Dangolani S, Panahi F, Tavaf Z, Nourisefat M, Yousefi R, Khalafi-Nezhad A. Synthesis and Antioxidant Activity Evaluation of Some Novel Aminocarbonitrile Derivatives Incorporating Carbohydrate Moieties. *ACS Omega.* 2018;3(8):10341–10350.  
<https://doi.org/10.1021/acsomega.8b01124>.
20. Paliwal PK, Jetli SR, Jain S. Green approach towards the facile synthesis of dihydropyrano(c)chromene and pyrano[2,3-*d*]pyrimidine derivatives and their biological evaluation. *Med Chem Res.* 2013;22(6):2984–2990. <https://doi.org/10.1007/s00044-012-0288-3>.
21. Kalaria PN, Satasia SP, Raval DK. Synthesis, characterization and biological screening of novel 5-imidazopyrazole incorporated fused pyran motifs under microwave irradiation. *New J Chem.* 2014;38(4):1512–1521. <https://doi.org/10.1039/C3NJ01327H>.
22. Agalave SG, Maujan SR, Pore VS. Click Chemistry: 1,2,3-Triazoles as Pharmacophores. *Chem Asian J.* 2011;6(10):2696–2718. <https://doi.org/10.1002/asia.201100432>.
23. Dheer D, Singh V, Shankar R. Medicinal attributes of 1,2,3-triazoles: Current developments. *Bioorg Chem.* 2017;71:30–54. <https://doi.org/10.1016/j.bioorg.2017.01.010>.
24. Shaikh MH, Subhedar DD, Nawale L, et al. 1,2,3-Triazole derivatives as antitubercular agents: synthesis, biological evaluation and molecular docking study. *MedChemComm.* 2015;6(6):1104–1116. [10.1039/C5MD00057B](https://doi.org/10.1039/C5MD00057B).
25. Yu J-L, Wu Q-P, Zhang Q-S, Liu Y-H, Li Y-Z, Zhou Z-M. Synthesis and antitumor activity of novel 2',3'-dideoxy-2',3'-diethanethionucleosides bearing 1,2,3-triazole residues. *Bioorg Med Chem Lett.* 2010;20(1):240–243. <https://doi.org/10.1016/j.bmcl.2009.10.127>.
26. Giffin MJ, Heaslet H, Brik A, et al. A Copper(I)-Catalyzed 1,2,3-Triazole Azide–Alkyne Click Compound Is a Potent Inhibitor of a Multidrug-Resistant HIV-1 Protease Variant. *J Med Chem.* 2008;51(20):6263–6270. <https://doi.org/10.1021/jm800149m>.

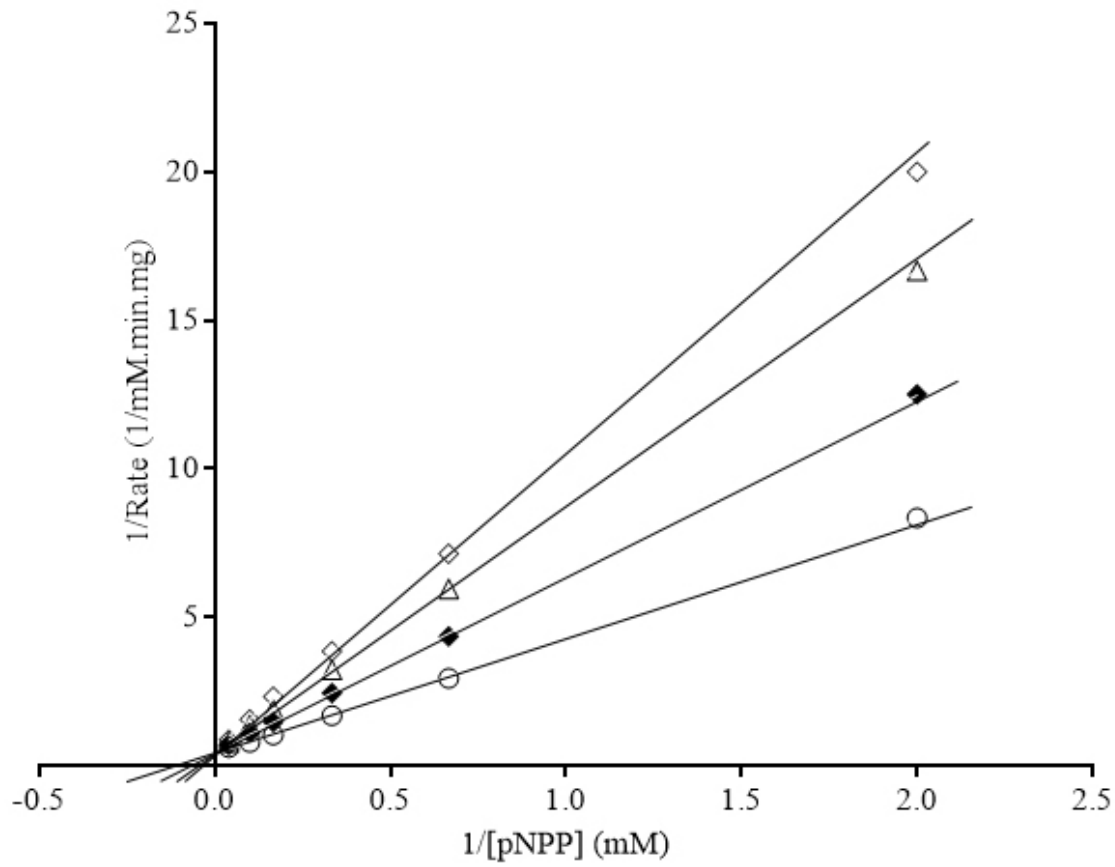
27. Buckle DR, Rockell CJM, Smith H, Spicer BA. Studies on 1,2,3,-triazoles. 10. Synthesis and antiallergic properties of 9-oxo-1H,9H-benzothiopyrano[2,3-d]-1,2,3-triazoles and their S-oxides. *J Med Chem.* 1984;27(2):223–227. <https://doi.org/10.1021/jm00368a021>.
28. Guantai EM, Ncokazi K, Egan TJ, et al. Design, synthesis and in vitro antimalarial evaluation of triazole-linked chalcone and dienone hybrid compounds. *Biorg Med Chem.* 2010;18(23):8243–8256. <https://doi.org/10.1016/j.bmc.2010.10.009>.
29. Sangshetti JN, Nagawade RR, Shinde DB. Synthesis of novel 3-(1-(1-substituted piperidin-4-yl)-1H-1,2,3-triazol-4-yl)-1,2,4-oxadiazol-5(4H)-one as antifungal agents. *Bioorg Med Chem Lett.* 2009;19(13):3564–3567. <https://doi.org/10.1016/j.bmcl.2009.04.134>.
30. Pokrovskaya V, Belakhov V, Hainrichson M, Yaron S, Baasov T. Design, Synthesis, and Evaluation of Novel Fluoroquinolone–Aminoglycoside Hybrid Antibiotics. *J Med Chem.* 2009;52(8):2243–2254. <http://doi.org/10.1021/jm900028n>.
31. Zhou B, He Y, Zhang X, et al. Targeting mycobacterium protein tyrosine phosphatase B for antituberculosis agents. *Proc Natl Acad Sci U S A.* 2010;107(10):4573–4578. <https://doi.org/10.1073/pnas.0909133107>.
32. Tan LP, Wu H, Yang P-Y, et al. High-Throughput Discovery of Mycobacterium tuberculosis Protein Tyrosine Phosphatase B (MptpB) Inhibitors Using Click Chemistry. *Org Lett.* 2009;11(22):5102-5105. <https://doi.org/10.1021/ol9023419>.
33. Chittepu P, Sirivolu VR, Seela F. Nucleosides and oligonucleotides containing 1,2,3-triazole residues with nucleobase tethers: Synthesis via the azide-alkyne ‘click’ reaction. *Biorg Med Chem.* 2008;16(18):8427–8439. <https://doi.org/10.1016/j.bmc.2008.08.026>.
34. Gupte A, Boshoff HI, Wilson DJ, et al. Inhibition of Siderophore Biosynthesis by 2-Triazole Substituted Analogues of 5'-O-[N-(Salicyl)sulfamoyl]adenosine: Antibacterial Nucleosides Effective against Mycobacterium tuberculosis. *J Med Chem.* 2008;51(23):7495–7507. <https://doi.org/10.1021/jm8008037>.

35. Kumar KK, Seenivasan SP, Kumar V, Das TM. Synthesis of quinoline coupled [1,2,3]-triazoles as a promising class of anti-tuberculosis agents. *Carbohydr Res.* 2011;346(14):2084–2090.  
<https://doi.org/10.1016/j.carres.2011.06.028>.
36. Bhat AR, Dongre RS, Naikoo GA, Hassan IU, Ara T. Proficient synthesis of bioactive annulated pyrimidine derivatives: A review. *J Taibah Univ Sci.* 2017;11(6):1047–1069.  
<https://doi.org/10.1016/j.jtusci.2017.05.005>.
37. Mollashahi E, Nikraftar M. Nano-SiO<sub>2</sub> catalyzed three-component preparations of pyrano[2,3-*d*]pyrimidines, 4*H*-chromenes, and dihydropyrano[3,2-*c*]chromenes. *J Saudi Chem Soc.* 2018;22(1):42–48. <https://doi.org/10.1016/j.jscs.2017.06.003>.
38. Boda SK, Pishka V, Lakshmi PVA, Chinde S, Grover P. 1,2,3-Triazole Tagged 3*H*-Pyrano[2,3-*d*]pyrimidine-6-carboxylate Derivatives: Synthesis, in Vitro Cytotoxicity, Molecular Docking and DNA Interaction Studies. *Chem Biodivers.* 2018;15(6):e18000101.  
<https://doi.org/10.1002/cbdv.201800101>.
39. Copeland RA. Evaluation of Enzyme Inhibitors in Drug Discovery: A Guide for Medicinal Chemists and Pharmacologists. Second Edition ed.: John Wiley and Sons; 2013:25–95.
40. Guo X-L, Shen K, Wang F, Lawrence DS, Zhang Z-Y. Probing the Molecular Basis for Potent and Selective Protein-tyrosine Phosphatase 1B Inhibition. *J Biol Chem.* 2002;277(43):41014–41022.  
<https://doi.org/10.1074/jbc.M207347200>.
41. Grundner C, Perrin D, Hooft van Huijsduijnen R, et al. Structural Basis for Selective Inhibition of *Mycobacterium tuberculosis* Protein Tyrosine Phosphatase PtpB. *Structure.* 2007;15(4):499–509.  
<https://doi.org/10.1016/j.str.2007.03.003>.

Compound **8v**

ACCEPTED

## Compound 8x



ACCEPTED

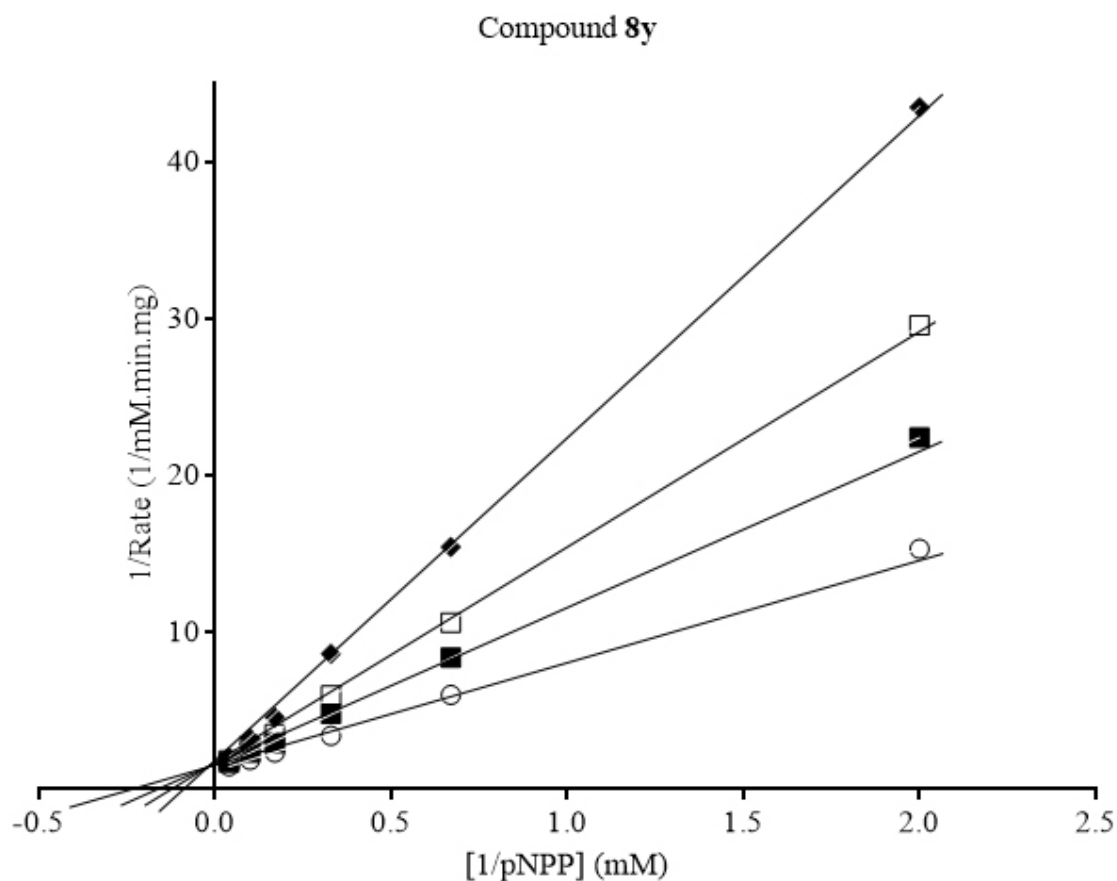


**Figure 3.** Competitive inhibitory profile of the most active compounds **8v**, **8x**, and **8y**. Lineweaver-Burk double-reciprocal plots represented inhibitory profiles of these compounds against MtbPtpB. Kinetic experiments were conducted in the presence of increasing concentrations of inhibitors: 0  $\mu\text{M}$  ( $\circ$ ), 1  $\mu\text{M}$  ( $\blacksquare$ ), 1.5  $\mu\text{M}$  ( $\square$ ), 2  $\mu\text{M}$  ( $\blacklozenge$ ), 3  $\mu\text{M}$  ( $\triangle$ ), 4  $\mu\text{M}$  ( $\diamond$ ); *p*NPP was used as substrate in all experiments.

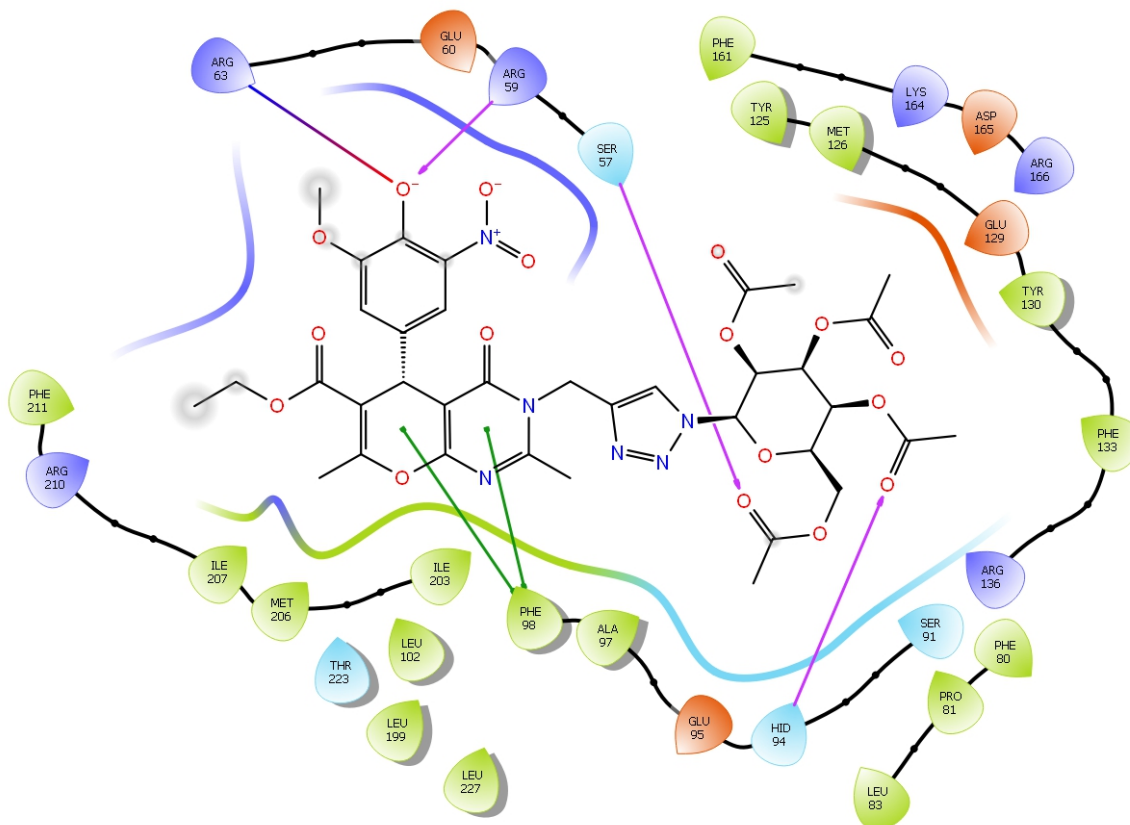


**Figure 4.** Amino acids involved in intermolecular interactions of 1H-1,2,3-triazole **8y**.

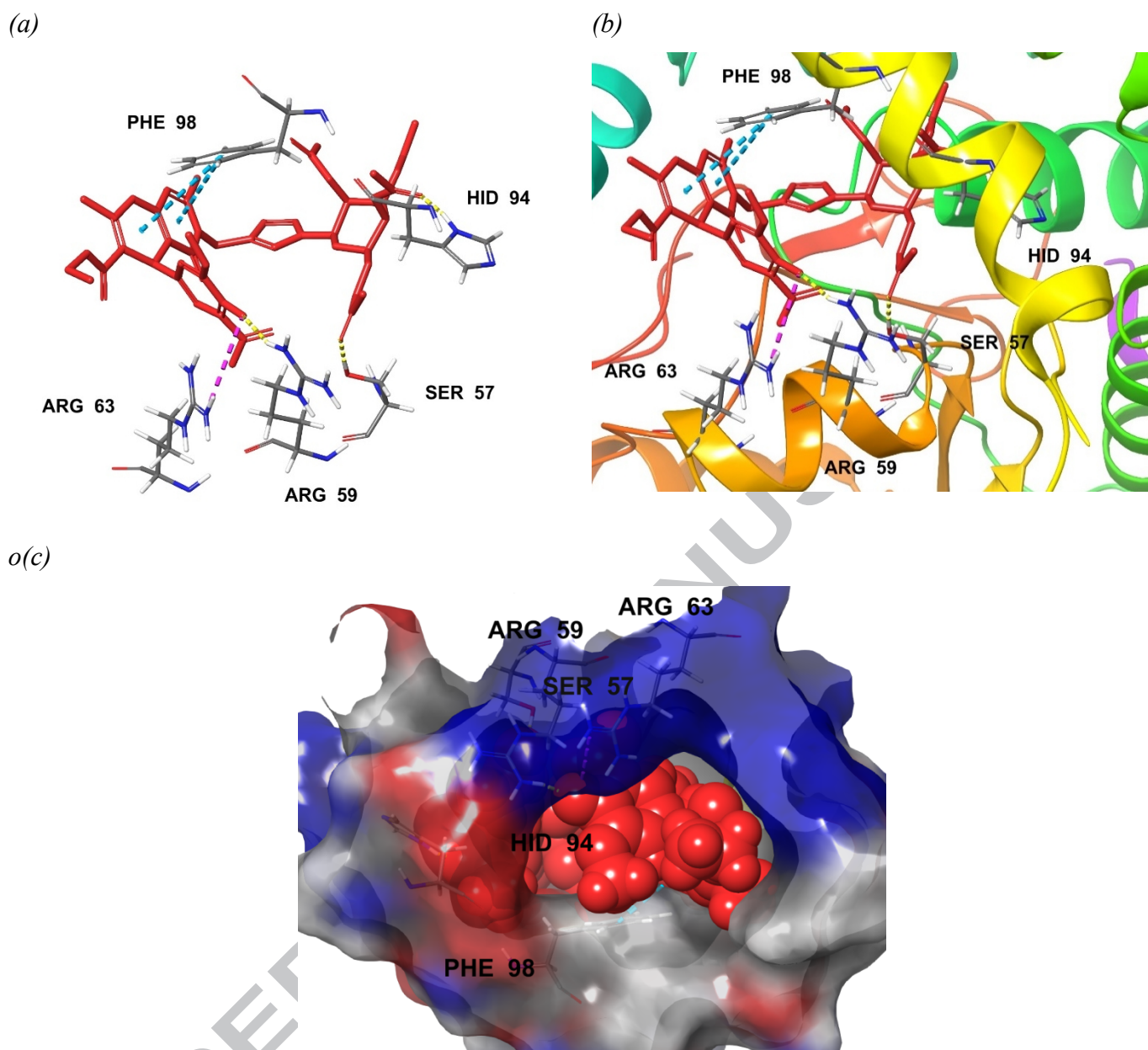


**Figure 5.** (a,b) Compound **8y** (in red color) in MTB phosphotyrosine phosphatase B protein (PDB ID: 2OZ5). (c) Alignment of compound **8y** in the binding pocket (in residue-charge color scheme).

### Highlights

- Novel thirty-four 1*H*-1,2,3-triazole-tethered 4*H*-chromene–D-glucose conjugates
- **8g**, **8t**, **8u**, **8v**, **8x**, and **8y**: inhibitory activity  $IC_{50}$ =1.56–9.52  $\mu$ M against MtbPtpB
- Ser57, Arg59, Hid94, and Phe98 residues of 2OZ5 created the specific binding pocket

## Graphic abstract

